A project for climatologic mapping of soil water content in Trentino

Emanuele Eccel[1*], *Emanuele Cordano*[1], *Fabio Zottele*[2]

Abstract: *Project IdroClima had the aim of studying the high-resolution (500 m) water content of Trentino soils under a climatological perspective. The water budget model GEOtop 2.0 was applied to a 21-year period (1992-2012), corresponding to the hourly coverage of meteorological data. GEOtop accepts a thorough meteorological input, including several atmospheric variables. Pedology was described with a uniform soil over the domain, with 9 theoretical layers. Soil use was input according to the CORINE Land Cover classes. A qualitative validation of the model was done with pre-existent probe measurements of soil moisture (2006 - 2008) and with comparison with measured data from weather stations. A thorough set of post-processing was carried out, to consider several possible aggregation algorithms for daily maps. The main results are analyzed and discussed in this work. The simulation shows geographical patterns of proneness to drought or to proximity with a wider water availability, according to areas.*
Keywords: *soil water content, soil moisture, GEOtop, Trentino, climate.*

Riassunto: *Il progetto IdroClima ha la finalità di simulare il contenuto d'acqua nei suoli del Trentino ad elevata risoluzione spaziale (500 m) secondo una prospettiva climatologica. Il bilancio idrico del modello GEOtop 2.0 è stato applicato ad un periodo di 21 anni (1992-2012), corrispondente al periodo di disponibilità del dato meteorologico orario. GEOtop accetta un input meteorologico completo, includendo diverse variabili atmosferiche. La pedologia è stata descritta con un suolo uniforme sul dominio, con 9 strati teorici. L'uso del suolo è stato inserito secondo le classi di CORINE Land Cover. La validazione del modello è stata eseguita qualitativamente mediante misure pre-esistenti di umidità del suolo (2006 – 2008) e con il confronto con dati misurati da stazioni meteorologiche. È stata eseguita un'ampia post-elaborazione del dato grezzo, per prendere in considerazione diversi possibili algoritmi di aggregazione per le mappe giornaliere. I risultati principali sono analizzati e discussi nel lavoro. La simulazione mostra, secondo le aree, pattern geografici di predisposizione alla siccità o alla prossimità con una più ampia disponibilità idrica.*
Parole chiave: *contenuto idrico dei suoli, umidità dei suoli, GEOtop, Trentino, clima.*

1. INTRODUCTION

Water cycle from atmosphere down to vegetation cover and soil is strongly affected by the present - and expected - climate change (Spinoni *et al.*, 2014; Damberg and AghaKouchak, 2014). Particularly, temperature increase is expected to bring dramatic consequences for drought conditions, with an increase in water demand as a result of evapotranspiration (Sheffield and Wood, 2008a, 2008b). And, in general, different climate conditions show different resilience to climate change, the effect of single drivers having unequal effects on evapotranspiration (Tabari and Talaee, 2014). In any case, concern for an increasing trend is widespread in many Southern Europe and Mediterranean areas (Vicente-Serrano *et al.*, 2014). In northern Italy, and close to the area where this work was carried out (Trentino), the European Project LIFE + "Trust" has addressed measures to mitigate the impacts of climate change on the groundwater for agricultural needs (Bisaglia *et al.*, 2011). In Trentino, the impacts of climate change on the hydrologic cycle have not been extensively investigated; Grossi *et al.*, (2013) studied vulnerability of a regional glacier to climate change, while collaborative European projects have been devoted to the investigation of impacts to areas including Trentino: ORIENTGATE, focusing on the adaptation in water management in a changing climate (http://www.orientgateproject.org/), and CLIMB (Climate Induced Changes on the Hydrology of Mediterranean Basins - http://www.climb-fp7.eu/), which considered Noce river catchment in Trentino. But, more in general, the assessment of climate change on water cycle is crucial for the adaptation to its impacts. Seneviratne *et al.*, (2010) have reviewed the state of the art on the knowledge of interplay

* Corresponding author's e-mail: emanuele.eccel@fmach.it
[1] Sustainable Agro-ecosystems and Bioresources Department, IASMA Research and Innovation Centre, Fondazione Edmund Mach, 38010 San Michele all'Adige, (TN), Italy.
[2] Technological Transfer Centre, Fondazione Edmund Mach, 38010 San Michele all'Adige, (TN), Italy.
Received 19 August 2014, accepted 05 October 2014.

between soil moisture and the general climate system, considering also how soil water content affects climate change.

An assessment of soil water content can be tackled with different approaches; Ford and Quiring (2014) have applied time interpolation methods to a general network of measurements; this can be done in presence of records of desired duration for the study area. Some data could be supplied from the Global Soil Moisture Network (previously: GSM Data Bank - Robock *et al.*, 2000). However, the required resolution and observation periods are seldom available for the wanted target areas; in this case, assessments based on satellite measurements have been proposed, and such an approach typically applies to large scale estimations, like the global scale (Damberg and AghaKouchak, 2014); nonetheless, results may not agree with others from different sources.

In Italy, Cicogna *et al.*, (2008) simulated water balance for agro-climatological purposes, producing a sub-regional map in Friuli – Venezia Giulia for a long reference period, making use of 10-day weather series. Likewise, in the frame of the wider project of Climate Atlas of Trentino, the availability of data and maps on the water content in soils, under a climatological perspective, addresses a still poorly investigated issue in the environmental and agro-ecosystem sector.

2. METHODS

2.1. The model in general

The assessment of water content can be known by solving two balance equations: water balance (conservation of water mass) and energetic balance (conservation of energy). There are models that allow the solution of such equations by considering weather conditions, soil properties, and soil cover features. In this study, the water balance processing was carried out by the hydrological model "GEOtop". This model was started in 1999 thanks to a co-funding by the Autonomous Province of Trento and the Ministry for University and Research. Since then, the model was developed, up to the present 2.0 version, used in this work. A thorough discussion can be found in Endrizzi *et al.*, (2011), and particularly in Endrizzi *et al.*, (2013) for the upgraded version 2.0. Also Rigon *et al.*, (2006) described in detail many aspects of the physics implemented in the model.

GEOtop is a physically-based model which analyses the whole hydrological cycle on a water catchment. The model accepts as input the topographic features (digital terrain model), which are processed to yield useful indices for the calculation of the water balance, such as slope, aspect, shading, sky view factor.

GEOtop represents a powerful tool for the simulation of:

- soil water content;
- soil evaporation;
- vegetation transpiration;
- snow dynamics in the basin;
- surface temperature in the basin;
- soil and bedrock temperature, even under frost conditions;
- glacier mass balance;
- water table depth and interaction with snow and ice melting;
- river rate of flow in the basin.

The hydrologic features of soil, detailed over a number of vertical levels, enter the model input to simulate water infiltration and runoff.

Soil use classes are part of GEOtop's input. They are treated according to a double layer scheme (Endrizzi and Marsh, 2010), allowing to separate the contribute of vegetation from that of surface on turbulent fluxes. The scheme of soil use and vertical layout of soil is given in Fig. 1.

Weather data are the fundamental input for water balances. They are spatially interpolated on the geographic domain with the model Micromet (Liston and Elder, 2006). Hence, the model calculates the energy and mass balances in the catchment basin by a 3D solver for the Richards' equation and a 1D solver for the energy equation.

The snow module calculates accumulation and melting by a multilayer discretisation of the snowpack, which includes wind drift effects.

All water and energy fluxes between soil and atmosphere are treated at the boundary conditions. In particular, evapotranspiration is calculated as a water vapour turbulent flux (see equation 30 in Endrizzi *et al.*, 2014) and is proportional to the gradient of saturated specific humidity between soil and atmosphere through a coefficient depending on lower atmosphere turbulence and land-use classes:

$$LE = \beta_\gamma L_e \rho_a c_p W_s \frac{Q_a - \alpha_\gamma Q^*_{sur}}{r_a}$$

where LE is the latent heat, β_γ and α_γ are coefficients to take into account soil resistance to evaporation, L_e is the specific heat of vaporization, ρ_a is air density, c_p is the the specific heat at constant pressure, W_s is the wind speed, Q_a is the specific

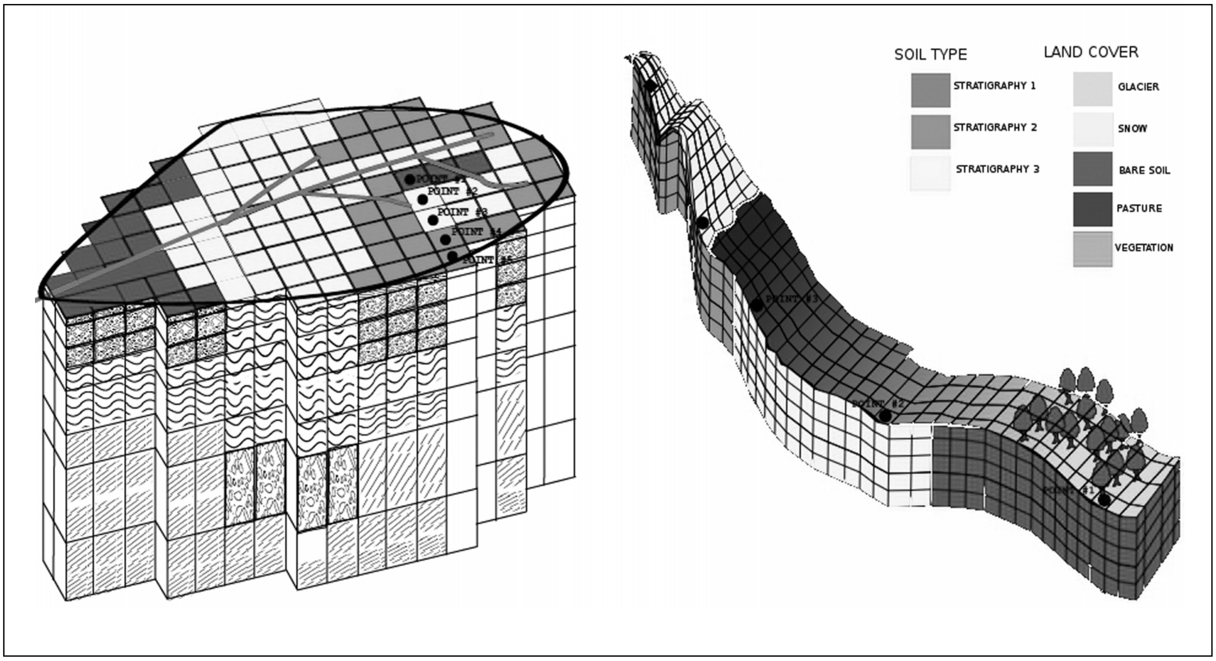

Fig. 1 - GEOtop: example of attribution of homogeneous soil use classes and pedological classes in the catchment domain. Every class is defined for all soil layers used (from Endrizzi *et al.*, 2011).
Fig. 1 - GEOtop: esempio di attribuzione di classi di uso del suolo e classi pedologiche omogenee nel dominio del bacino. Ogni classe è definita in tutti i livelli di suolo definiti (da Endrizzi et al.*, 2011).*

humidity of air, Q^{*}_{sur} is the saturated specific humidity, and r_a is the aerodynamic resistance. More details are found also in Bertoldi *et al*, 2010.
Once the soil use has been set at any grid point, all the features, useful for the evapotraspiration modelling, are defined. Among these, the most relevant (but the list is not complete) are:

- canopy fraction;
- vegetation height;
- root depth;
- vegetation cover density;
- stomatal resistance;
- soil reflectivity (both visible and near infrared).

2.2 Geographic features, soil use and climate of the study area

Trentino is a region in the central- eastern Italian Alps, which encompasses various climatic areas. Altitude ranges between 70 m a.s.l. to 3769 m of the Cevedale peak. This mountainous region contains a system of valleys converging in its central part on the largest and longest valley of Adige river. The latter is often deep, and has a flat bottom formed by alluvia from the River Adige.
The low-middle elevation climatic areas of Trentino can be ascribed to a Köppen "Cfb" class ("temperate, middle latitudes climate, with no dry season"). More elevated, mountain areas (covered by the weather station network) fall into a "Dfc" classification ("microthermal climate, humid all year round"). Trentino climate is mostly oceanic, with some areas showing features of transition to a more continental-alpine climate, cooler and often drier, more typical of the inner mountain valleys. Precipitation is mostly distributed over two maxima, in the autumn (main) and in the spring (secondary). In general, mountain areas have moister summer seasons (Eccel and Saibanti, 2007).
The spatial resolution for this work was set to 500 m. For the simulation, the calculation domain has been extended, with respect to the administrative limits of Trentino, to include also parts of the Adige and Sarca river catchment basins (Fig. 2).
Parameterisation of soil use affects both mass and energy balances, involving wind speed modelling, turbulence, and the splitting of evapotranspiration between soil and canopy. The GEOtop implementation has envisaged 11 soil use classes, assigned according to the similarity with the classes of the two following sources:

- for Trentino: soil use maps from the OpenData Trentino [*http://dati.trentino.it*], from model CORINE;

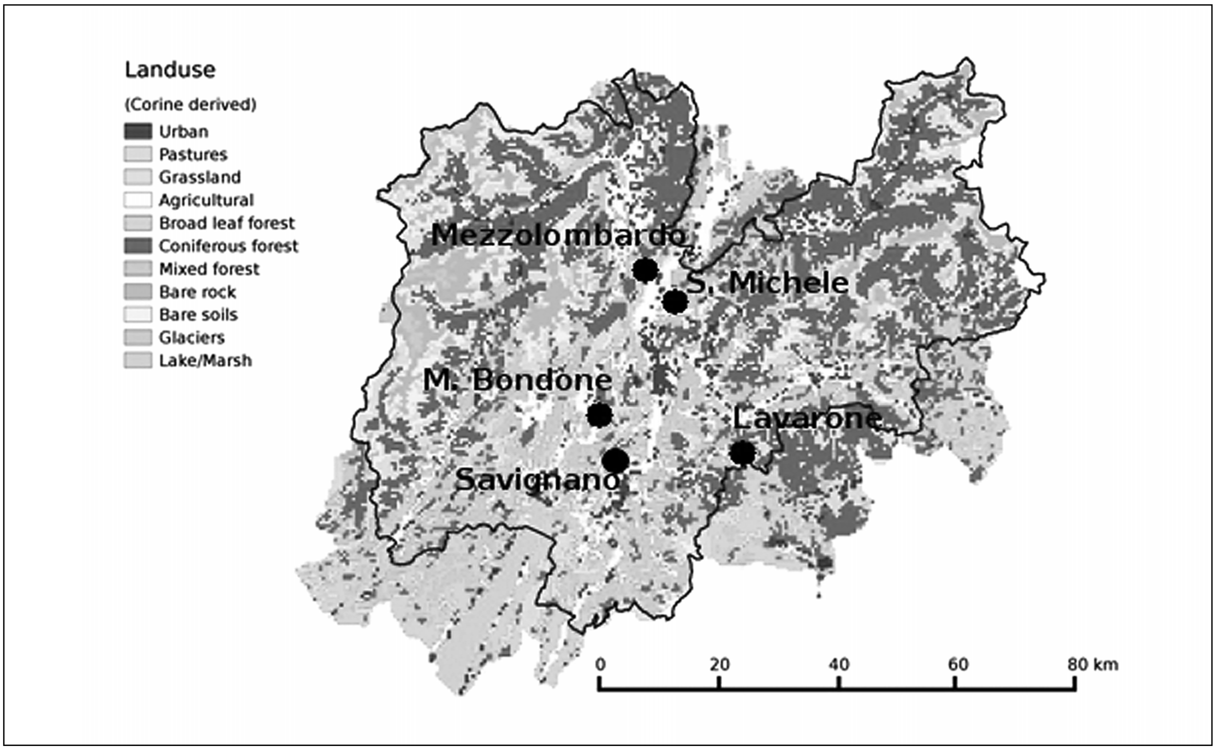

Fig. 2 - The used soil use map (from CORINE land use) with the five control sites
Fig. 2 - Mappa di uso del suolo impiegata (da CORINE land use) con i cinque punti di controllo.

- for the bordering areas: maps of CORINE Land Use (Reuter *et al.*, 2007; Jarvis *et al.*, 2008).

The land use categories used in this application of GEOtop are the following:

1. Urban
2. Pasture
3. Grassland
4. Agricultural
5. Broad leaf forest
6. Coniferous forest
7. Mixed forest
8. Bare Rocks
9. Bare Soils
10. Glacier
11. Lake/Marsh.

The GEOtop configuration file contains all utilized values for physical parameters required for the description of turbulent fluxes in function of such land use categories.

2.3 Meteorological input

The meteorological input admitted by GEOtop is exhaustive, including the following quantities:

– precipitation
– wind velocity and direction
– relative humidity
– dew point temperature
– air temperature
– atmospheric pressure
– global (shortwave) radiation (also direct, diffuse and net)
– long wave radiation.

GEOtop also admits the setting of altitudinal gradients of temperature, precipitation, and dewpoint temperature.

The meteorological data used for the calculation of balances came from 126 weather stations and have been supplied by Meteotrentino (Autonomous Province of Trento) and Fondazione E. Mach – Geographic Information System Unit, San Michele all'Adige. Data were aggregated on an hourly basis, being this the time step used for hydrological simulations in GEOtop.

2.4 Infiltration modelling

In GEOtop, every cell in the domain can be identified by a pedological category, defined as in the example of Tab. 1 and Fig. 1.

The water content has been assessed at 9 different layers at growing depths, according to Tab. 2. However, due to the decreasing conductivity, practically blocking water infiltration, the

Stratigraphy ID	Layer ID involved	Soil texture
1	1,2,3	gravel
1	4,5	clay
1	6,7,8	sand
2	1	clay
2	2,3,4	gravel
2	5,6	clay
2	7,8	sand
3	1,3,4,5,6	clay
3	7	gravel
3	8	sand

Tab. 1 - Example of pedological classification in GEOtop (from Endrizzi *et al.*, 2011).
Tab. 1 - Esempio di classificazione pedologica in GEOtop (da Endrizzi et al.*, 2011).*

Layer number	Mean depth (cm)	Thickness (cm)
1	1.5	3
2	8	10
3	23	20
4	58	50
5	143	120
6	353	300
7	753	500
8	1603	1200
9	3453	2500

Tab. 2 - The soil layers used, their average thickness, and the corresponding mean depths.
Tab. 2 - Gli strati di suolo impiegati, spessori medi e profondità medie.

deepest layers were not considered in the analysis. Layers at depths greater than 1.5 m do not necessarily represent a physical reality of soil, but are simply functional to the simulation. The attribution of an extremely low hydraulic conductivity to a deep layer corresponds to simulate the presence of bed rock.
From this scheme, conductivity values (both vertical and horizontal) have been introduced. Hydric retention has been input according to parametric curves defined by van Genuchten parameters (Van Genuchten, 1980; Mualem, 1976). The parameters of these curves depend on toil texture and organic content. Some representative values are commented by works like Barontini *at al.*, (2005) and Cordano (2006). Such values model the retention and the hydraulic conductivity curves, that is, the functional link between volumetric water content in soil and interstitial pressure load or hydraulic conductivity, respectively. These curves are necessary for the closure (and then, the resolution) of Richards' equation, used in the soil water balance. The sub-surface flow is assumed to be almost linearly dependent on the piezometric gradient by a coefficient, called hydraulic conductivity, in turn dependent on soil permeability and from the instantaneous water content.
Since detailed information on soils in the region are missing, a "sandy clay loam" soil profile was chosen, adopting the values for the parameters of each soil layer given in Tab. 3.

Layer nr.	Dz	Kh	Kv	res	sat	a	n
1	30	0.1	0.1	0.08	0.5	0.004	1.3
2	100	0.1	0.1	0.08	0.5	0.004	1.3
3	200	0.05	0.05	0.08	0.5	0.004	1.3
4	500	0.05	0.05	0.08	0.5	0.004	1.3
5	1200	0.05	0.05	0.08	0.5	0.004	1.3
6	3000	0.001	0.001	0.08	0.5	0.004	1.3
7	5000	0.0001	0.0001	0.08	0.5	0.004	1.3
8	12000	0.0001	0.0001	0.08	0.5	0.004	1.3
9	25000	0.0001	0.0001	0.08	0.5	0.004	1.3

Legend:
Dz: layer thickness (mm)
Kh: normal (horizontal) hydraulic conductivity (mm s^{-1})
Kv: vertical hydraul ic conductivity (mm s^{-1})
res: residual water content (% vol.)
sat: saturation water content (% vol.)
a: parameter "a" in Van Genuchten curves (mm^{-1})
n: parameter "n" in Van Genuchten curves (-)

Tab. 3 - Soil hydrological features for GEOtop simulation.
Tab. 3 - Caratteristiche idrologiche del suolo impostate nella simulazione di GEOtop.

2.6 Data processing of GEOtop's output

GEOtop's distributed output was considered in this study. For some control point, singular series were extracted from the distributed output. In general, this was useful for validating results and particularly for the sites where soil moisture was measured for some periods. The only available measurements, located outside of the irrigation area, were two points where discontinuous measures were carried out between 2007 and 2008. The measurements were done at several soil depths with Sentek "Enviroscan" capacitive probes at Mezzolombardo (100 cm probe) and at San Michele all'Adige (50 cm probe), both in the Rotaliana Plain (see position in Fig. 2, which also represents positions of the sites where simulations were processed to extract point time series).

GEOtop's raw output consists in daily maps, one raster for each soil depth (3D variables). In this study, we only dealt with the volumetric liquid content and the interstitial pressure load as 3D variables. Other 2D variables were only considered for control purposes and are not discussed.

Daily maps were aggregated monthly, considering the following functions:

– mean
– minimum
– maximum
– 10^{th}, 50^{th}, 90^{th} percentiles.

One second aggregation level enables the analysis of the output according to a climatological time scale, aggregating monthly maps over years, with the same abovementioned functions.

It may be useful to consider anomaly maps referred to the average conditions of the whole area, as difference or ratio, with the following equations (referred to any raster point):

$$SW_{an} = SW - \overline{SW} \qquad SW_r = \frac{SW}{\overline{SW}}$$

where SW_{an} = anomaly (within map) of water content
SW = water content
$\overline{SW}$ = average water content for the whole map
SW_r = ratio (within map) between water content and average water content for the whole map.

From the absolute water content in soils (% volume) it is easy to pass to the value relative to the maximum available water content for the soil (% field capacity - % residual), or relative soil moisture:

$$SW_{rel} = \frac{SW - SW_{res}}{SW_{fc} - SW_{res}}$$

where SW_{rel} = relative water content (%)
SW = absolute volumetric water content (%)
SW_{fc} = volumetric water content at field capacity (%)
SH_{res} = residual volumetric water content (%).

All the post processing of output was carried out with the statistical software R (R Development Core Team, 2008). The geographical tools of R were used (*http://cran.r-project.org/*), particularly the libraries "raster" and "geotopbricks", the latter specially designed by E. Cordano *et al.*, for this purpose and contributed to the R-cran repository.

3. RESULTS

GEOtop simulation was run for 1990 - 2012, covering the period with availability of hourly data for the study area. To allow for a model stabilisation, and also considering the partial weather coverage for the early period, the analysis only considered years 1992 - 2012 (21 years), a period long enough to represent the present climatic conditions.

3.1 Model validation

For the model validation, the simulations have been verified at five points for the main control quantities: soil temperature, wind velocity, solar radiation, etc. In general, results are compatible with the reference measures, considering the resolution and the strong simplifications in the representation of topography, soil cover, and of the physical schematization of atmosphere.

In Fig. 3 the mean wind velocity is represented for the five control points, represented in Fig. 2. A good reproduction of seasonality can be seen, with realistic ratios between winter and summer, close to those measured by stations, as well as the effects of soil cover, which is parameterised by the typical height of the roughness objects (in the case of the five points, always trees).

In Fig. 4, soil temperature is represented at three different depths (8, 23, 58 cm). A verification was possible with the records of the San Michele station, where soil temperature are measured. An underestimation of about 2 °C can be detected, but with a correct estimation of seasonal thermal range. This underestimation affects soil icing, which penetrates at lower depths in the simulation, affecting also the layer nr. 4 (mean depth: 58 cm), and for periods longer than real for the other layers.

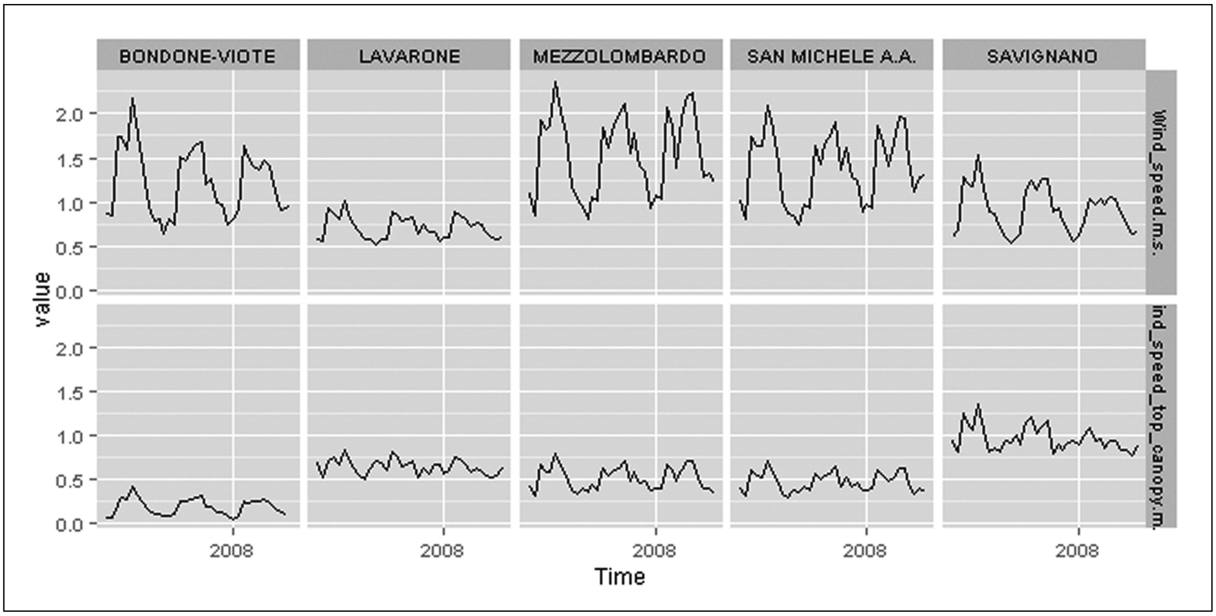

Fig. 3 - Simulations of mean wind velocity for the period 2006 – 2008 at five control positions. Upper panels: mean velocity. Lower panels: velocity above the canopy.
Fig. 3 - Simulazioni puntuali della velocità media del vento per il periodo 2006-2008 in cinque posizioni di controllo. Riquadri superiori: velocità media. Riquadri inferiori: velocità sopra la chioma delle piante.

In Fig. 5 the two components of the evapotranspirative flux are represented: from the canopy, due to the vegetation transpiration, and from soil (evaporation). The simulated values are well representative of the evapotranspiration regime typical for the regional climate. The differences, even important, among stations, can be ascribed to the different soil use (for the five points: broad-leaf forest [point 1], conifer forest [point 2], agricultural soil [points 3, 4, and 5].

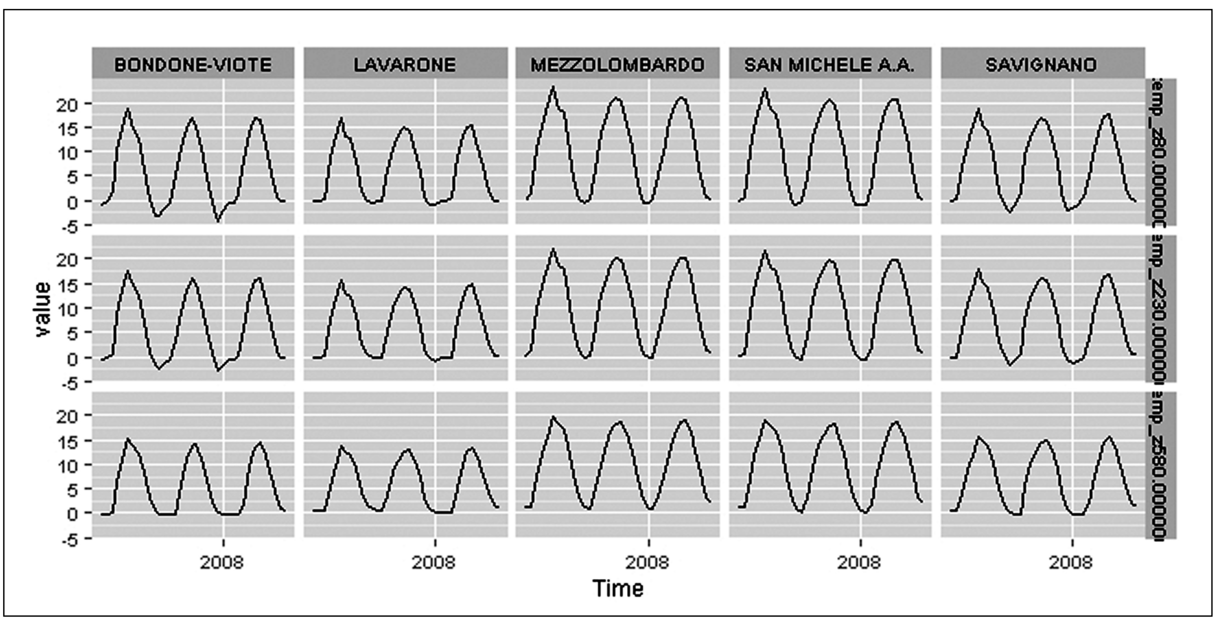

Fig. 4 - Point simulations of mean monthly soil temperature [°C] for the period 2006-2008 at five control positions. Upper line: mean depth of 8 cm. Second line: mean depth of 23 cm. Third line: mean depth of 58 cm.
Fig. 4 - Simulazioni puntuali della temperatura media mensile del suolo [°C] per il periodo 2006-2008 in 5 posizioni di controllo. Prima riga: profondità media di 8 cm. Seconda riga: profondità media di 23 cm. Terza riga: profondità media di 58 cm.

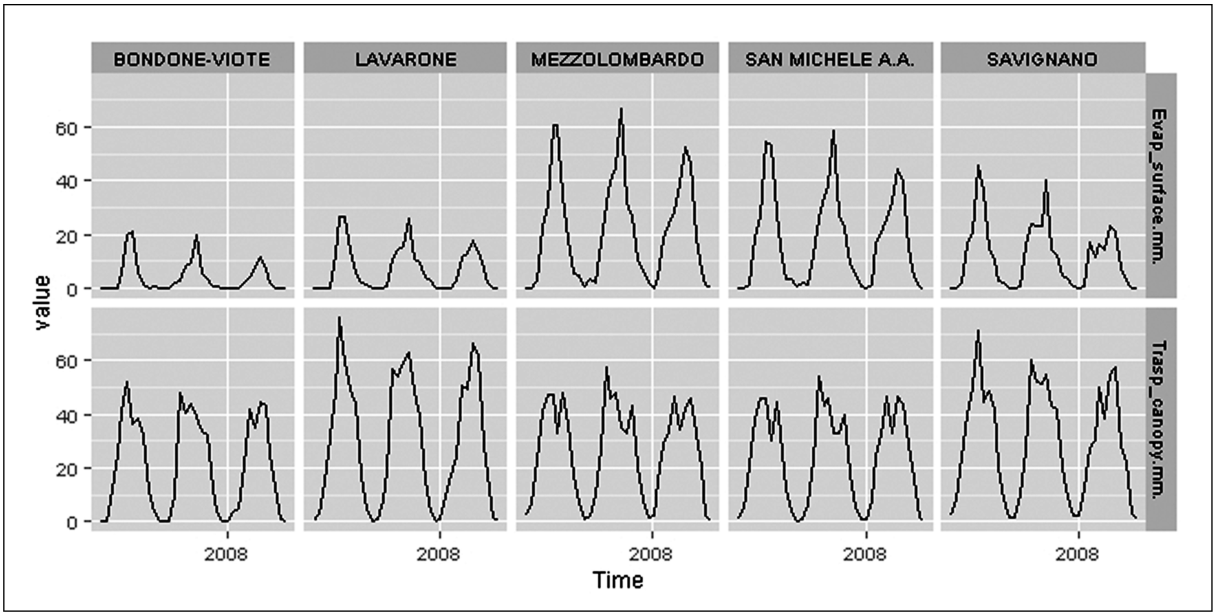

Fig. 5 - Point simulations of the two components of monthly evapotranspiration [mm] for the period 2006-2008 at five control positions. Upper line: soil evaporation. Lower line: canopy transpiration.
Fig. 5 - Simulazioni puntuali delle componenti di evapotraspirazione mensile [mm] per il periodo 2006-2008 in 5 posizioni di controllo. Riga superiore: evaporazione dal suolo. Riga inferiore: traspirazione dalla chioma.

The difference between two close stations, Mezzolombardo and San Michele, can be interpreted also considering that GEOtop assigns Mezzolombardo to the drainage area of the Rotaliana Plain - and, indeed, the Longobard suffix *"mezzo"* is perhaps to be ascribed to its ancient condition of boggy area before its reclamation.

The comparison of greater interest is, of course, with the measured soil moisture values.

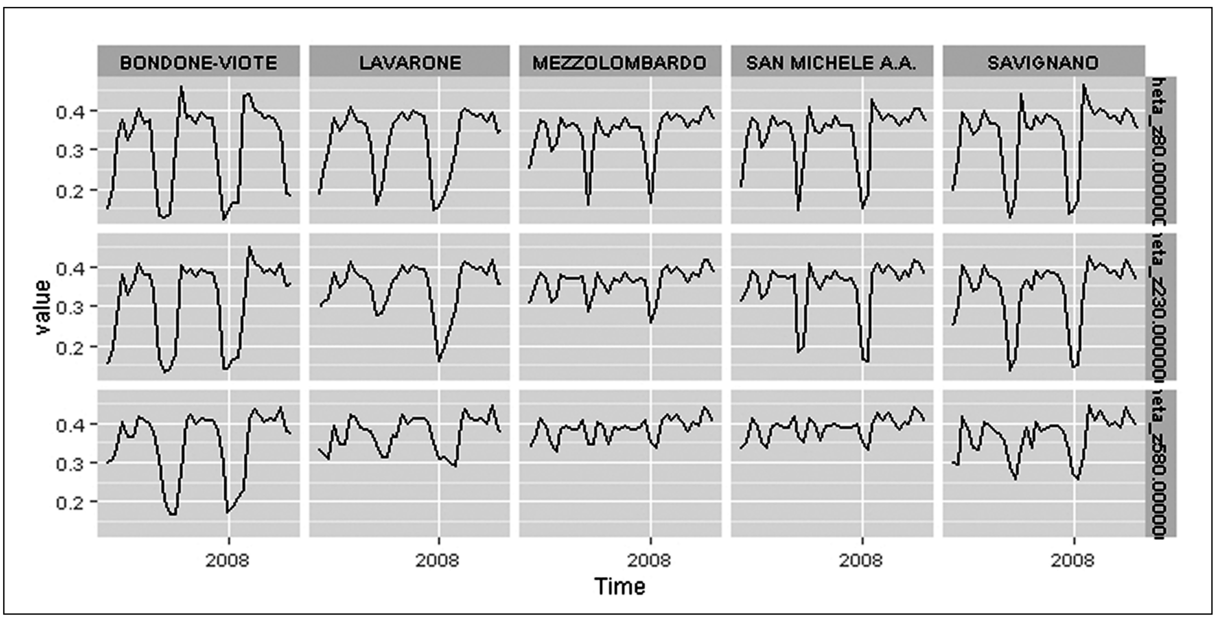

Fig. 6 - Point simulations of water content for the period 2006-2008 at five control positions, at three growing depths: 8 cm, 23 cm, 58 cm (mean layer depth).
Fig. 6 - Simulazioni puntuali del contenuto d'acqua per il periodo 2006-2008 in cinque posizioni di controllo, a tre profondità crescenti: 8 cm, 23 cm, 58 cm (profondità media dello strato).

Seneviratne *et al.*, (2010) pointed out the relevance of the presence of ground measures to validate soil moisture models, however coming to the conclusion that, in general, agreement between models and observations is mostly qualitative rather than quantitative.
Figg. 6 and 7 refer to relatively close sites, Mezzolombardo and San Michele, both lying on the floor of Rotaliana Plain, on the two opposite sides of Adige river. From Fig. 7, it can be seen that water content is strongly driven by hydraulic properties of soils, namely by retention curves at each depth. It can be also seen that water content dynamics is strongly attenuated at growing depths, having a quite stable trend already at 50 cm, and that seasonality is negligible with respect to the transients due to rainfall infiltration. The higher values in water content in the records are to be considered little reliable, probably owing to an incorrect instrument calibration. However, it can be seen that the model was capable of catching a significant increase of moisture corresponding to the rise measured in the spring 2008.
A direct comparison of model output with field measurements coming from the abovementioned records was done on pre-processed data. In order to address the unavoidable scale effects on absolute values, both measures and simulation were referred with respect to the minimum and maximum values in the series, respectively:

$$SW_{norm} = \frac{SW - SW_{min}}{SW_{max} - SW_{min}}$$

where SW_{norm} is soil water normalized to series extremes, SW is soil water (either measurements or model outputs), SW_{min} is minimum soil water content in the series, SW_{max} is maximum soil water content in the series. Results are reported in Fig. 8, where winter values have been omitted for the reasons explained in the following paragraph. Given the strong model simplifications, above all for the physical soil schematization, the comparison can be considered quite satisfactory in inferring signals from the simulations, of course with no claim to represent the true water content in any place and time.
In the seasonal trend of simulations, a recurring, abrupt lowering of soil moisture can be observed in the first two layers in winter, with no confirmation in measures. It is due to the different definitions of the quantities simulated by GEOtop, referring to the liquid water content, so that soil freezing has as a consequence the lowering of values down to the proximity to the residual, unavailable value of soil water.
Ultimately, the comparison of model output with existing measurements suggests to deal quantitative comparison of values with caution, at the same time qualitatively corroborating the results of the application of GEOtop.

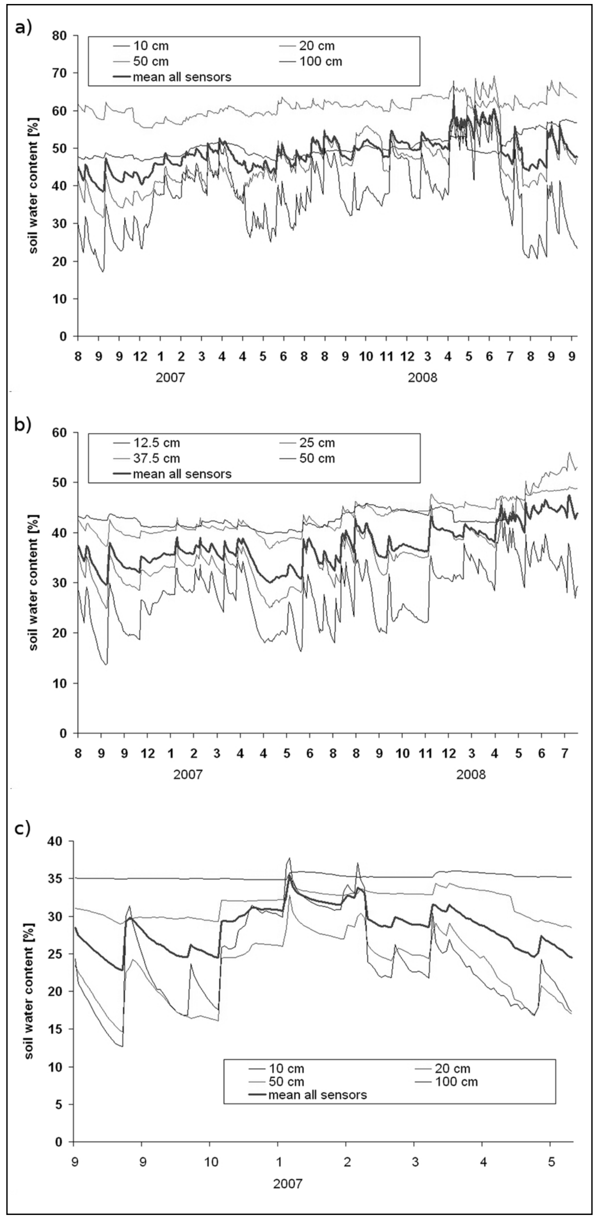

Fig. 7 - Volumetric soil moisture measures with capacitive probes – a) Mezzolombardo, 100 cm probe; b) Mezzolombardo, 50 cm probe; c) San Michele, 100 cm probe. Dark line is probe average, at any panel.
Fig. 7 - Misure volumetriche di umidità del suolo con sonde capacitive – a) Mezzolombardo, sonda da 100 cm; b) Mezzolombardo, sonda da 50 cm; c) San Michele, sonda da 100 cm. Medie delle misure in ogni riquadro: linea scura.

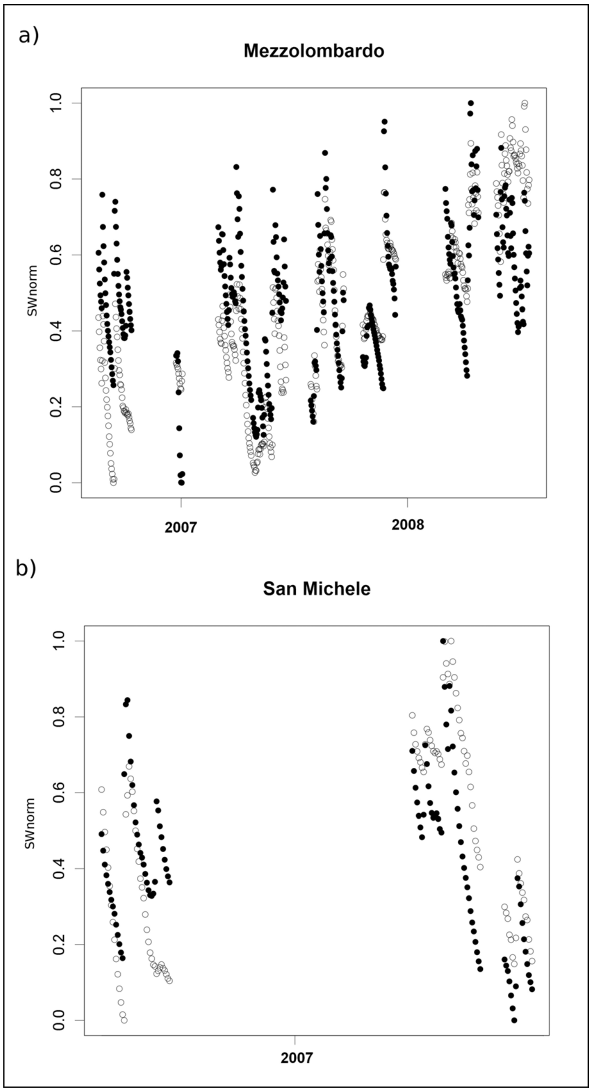

Fig. 8 - Normalized soil water content at two control points in Rotaliana Plain. Open dots: capacitive probe measurements; full dots: model simulations.

Fig. 8 - Contenuto d'acqua normalizzato in due punti di controllo in Piana Rotaliana.Punti bianchi: misure con sonde capacitive; punti neri: simulazioni di modello.

3.2 Processing, analysis and discussion of distributed model output

Several 3D-raster maps were processed and analysed. Results always refer to monthly aggregations in 1992 - 2012 (21 years). In detail, the following results have been analyzed:

– for soil water content:

- mean climatological water content (mean for several soil depths, monthly aggregated);
- minimum values;
- mean climatology of annual 10th percentiles of monthly minimums;

and these quantities were eventually processed to calculate:

- water content relative to the theoretical level of "available" water for soil;
- differences with respect to average map values;
- ratios with respect to average map values;
- shifts between different processing (e.g., comparison between mean and minimum values in the same period);

– for the hydraulic load:

- mean climatology of annual 10th percentiles of monthly minimums.

The number of possible combinations of this output design is extremely wide; for obvious space reasons, in this work only the more significant aspects will be discussed. Apart from few exceptions, the choice was done to represent one spring month (April) and one summer month (July), more representative than others for the water budget critical aspects, at a mean depth of 23 cm (layer nr. 3).

Fig. 9 represents the maps for three months of the year: January, April, and August. Winter values are, in general, determined by the presence of snow and frozen soil, which strongly hampers the dynamics of both temperature and soil content. The water content variable is relevant to the liquid portion only. Hence, winter maps have a comparative worth in the determination of aridity or drought conditions, except for analyses of high soil freezing (see also the point analysis at Sect. 3.1), which, during spring, can still take place and give place to events of physiologic aridity for forest plants (Montagnani *et al.*, 2005).

An average soil moisture regime is attained and maintained during summer. The resulting geographical pattern is strongly determined by orography, but also by typical rainfall regime in the region. These drivers determine the larger part of the variability of the soil water balance. Starting from the central part of the summer mean monthly values tend to stabilize, highlighting mountain, moister areas, as well as the zones more prone to water scarcity.

Well visible are the impluvium lines (valley bottoms), where the model simulates the drainage of infiltrated water. Sometimes the width of Adige valley allows the model to describe varied situations, not determined by the simple water flow, as occurs in smaller valleys and where, of course, saturation does not correspond to real hydrological soil conditions, but to the presence of a watercourse.

Fig. 10 is similar to Fig. 9, but the values, in this

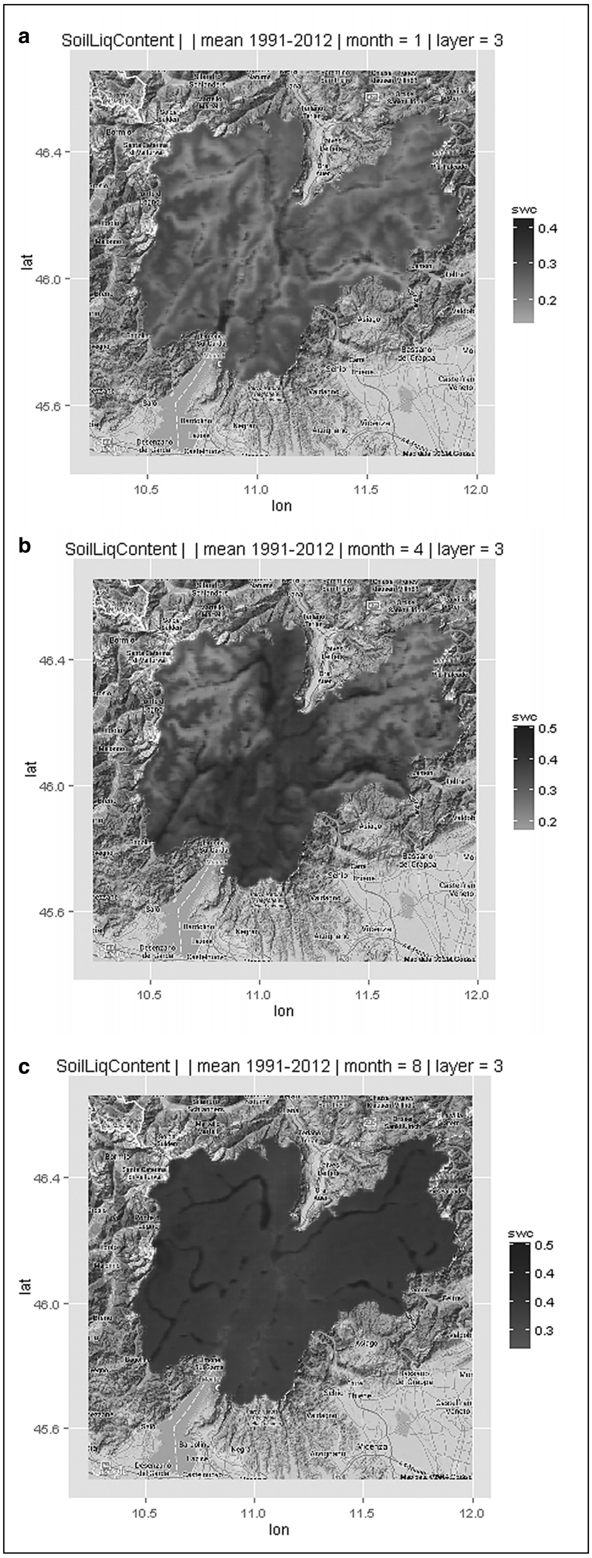

Fig. 9 - Mean volumetric soil water content at the average depth of 23 cm. Top to bottom: January, April, August
Fig. 9 - Contenuto medio volumetrico di acqua nel suolo alla profondità media di 23 cm. Dall'alto al basso: gennaio, aprile, agosto.

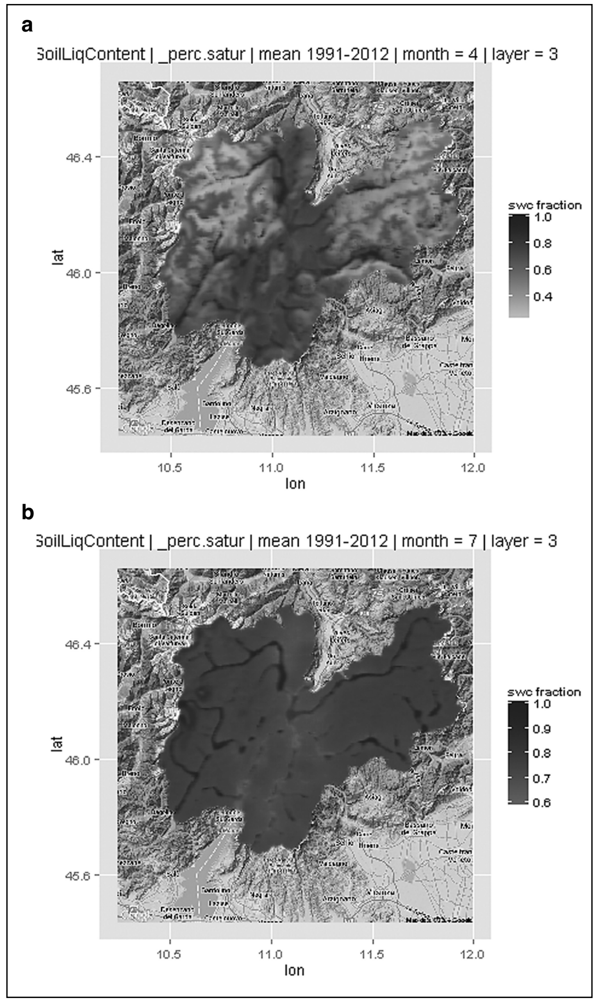

Fig. 10 - Average soil water content at the mean depth of 23 cm; values referred to the available water content (as fraction). Top: April. Bottom: July.
Fig. 10 - Contenuto medio di acqua nel suolo alla profondità media di 23 cm, valori riferiti al contenuto di acqua disponibile del suolo (frazione). Alto: aprile. Basso: luglio.

case, refer to the available water for the soils according to the retention curves. Such maps, if created with different soil classes, might reproduce a different pattern from that of the volumetric water content.
For an effective visualization, it can be useful to refer each map value to the average in the map itself. This was done in Fig. 11, where some patterns are highlighted, even not simply dependent on elevation and/or from territory morphology.
Fig. 12 shows the maps of a measure of low occurrence in soil moisture (annual 10th percentile of monthly minimums). This is a more robust estimator than the absolute minimum in

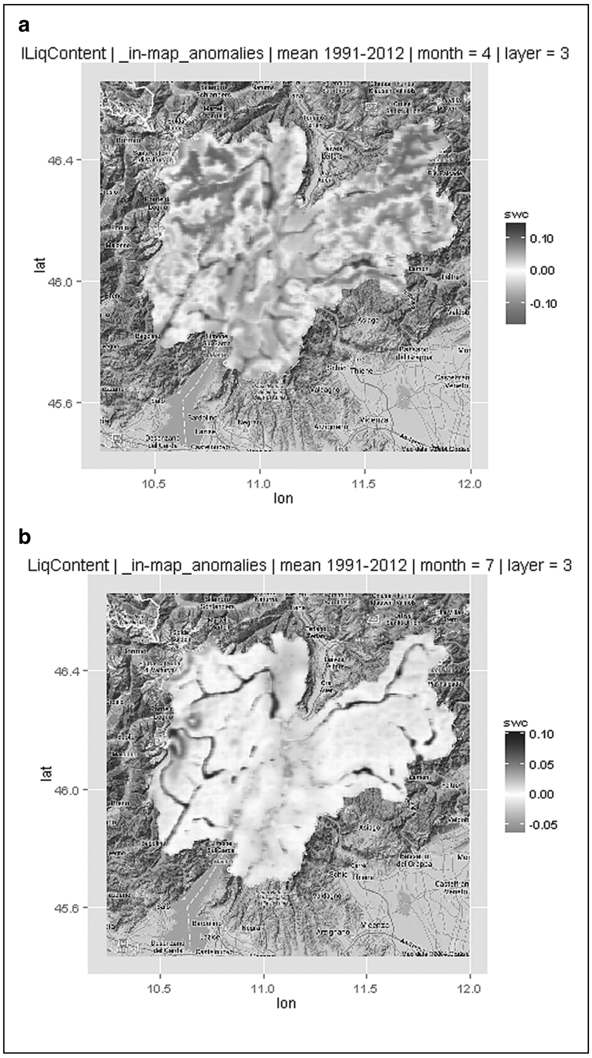

Fig. 11 - Like Fig. 9, but map of differences from the map average. Top: April. Bottom: July.
Fig. 11 - Come la Fig.9, mappa delle differenze con i valori medi di mappa. Alto: aprile. Basso: luglio.

the period, which can be affected by particularly rare events. It can be seen that mountain areas are less prone to summer droughts, given their typical rain regime, never too scarce in the warmer season.
As regards difference among layers, keeping in mind the hypothesis of uniform soil that was necessarily done, a good (theoretical) uniformity can be seen for the layers down to 58 cm of mean depth in the average climate conditions, that is, not considering the transients of rainfall wetting of soil. In Fig. 13 an example is given for the month of May.
Finally, it can be interesting to analyze the differences between minimum and typical (average) values for any month, in the same period. In Fig. 14 such difference is represented as anomaly within map. The most negative values show the areas more prone to a lowering of soil water content relative to the mean values in the same period. Particularly in summer months, such map shows the greater potential proneness of some areas to drought events.
Besides simulating soil water content, a useful check can be done on the pressure load, indicating the hydraulic load of water in soil, or, in other words, its depression, or water suction. This quantity has been analysed in particular in its minimum values, aggregated over years according

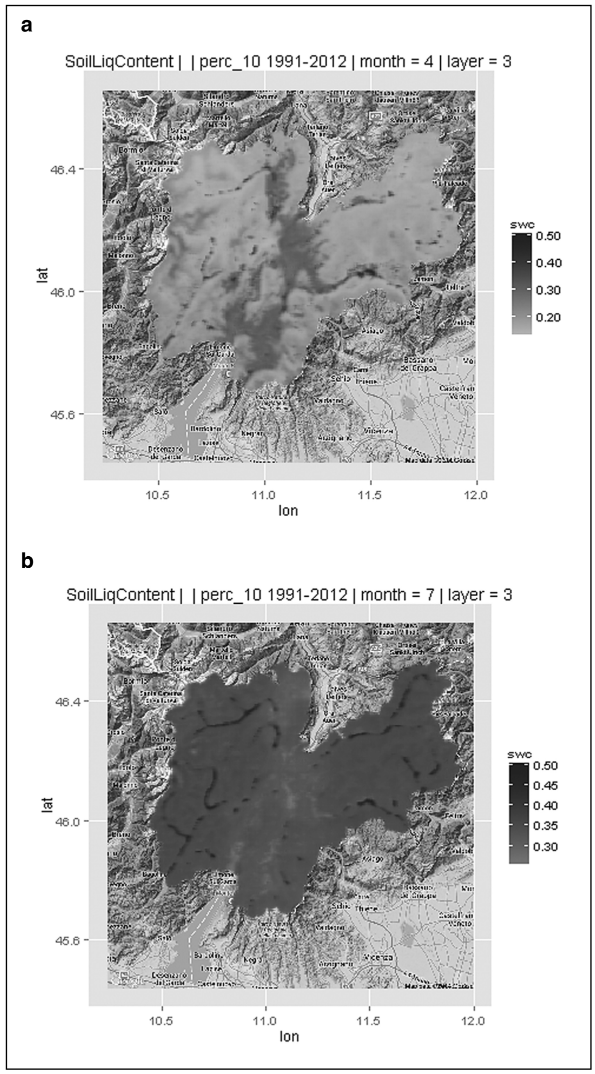

Fig. 12 - 10th annual percentile of monthly minimum of soil water content at the mean depth of 23 cm. Top: April. Bottom: July.
Fig. 12 - 10° percentile sugli anni dei minimi mensili del contenuto di acqua nel suolo alla profondità media di 23 cm. Alto: aprile. Basso: luglio.

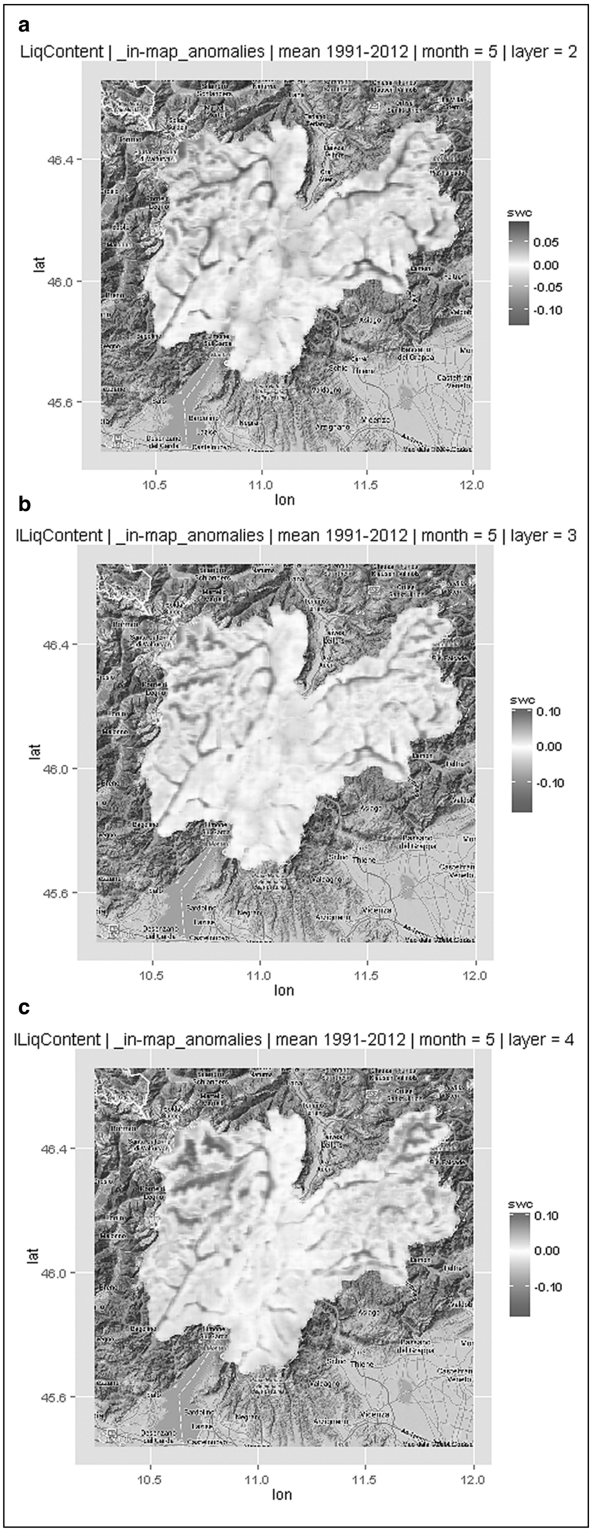

Fig. 13 - Mean soil water content at three depths (top to bottom: 8, 23, and 58 cm), month of May, anomalies with respect to mean map values.
Fig. 13 - Contenuto medio di acqua nel suolo a tre profondità (dall'alto al basso: 8, 23 e 58 cm), mese di maggio, anomalie rispetto ai valori medi di mappa.

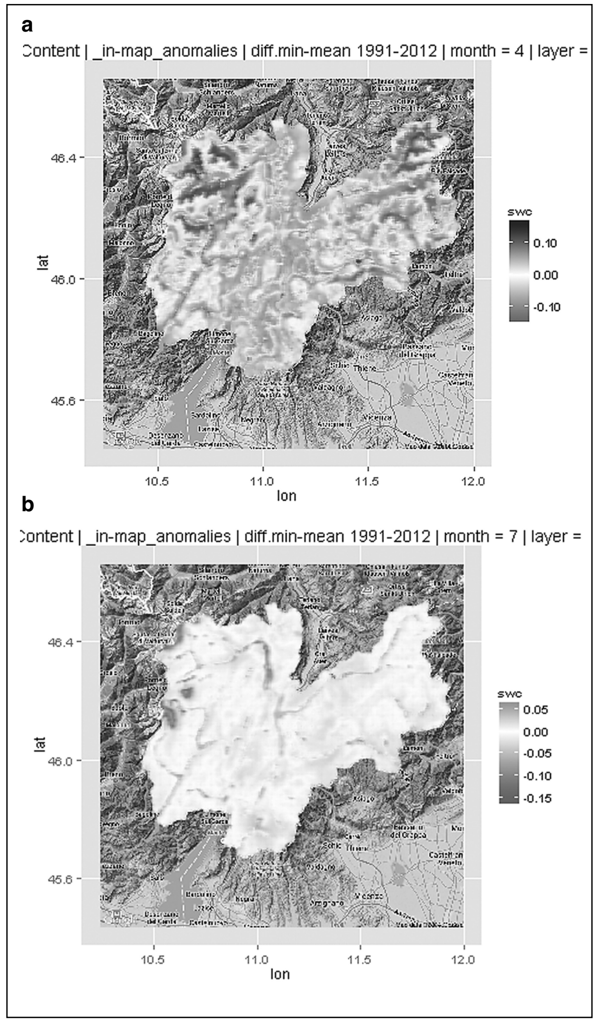

Fig. 14 - Difference between minimum and mean monthly values of soil water content at the mean depth of 23 cm, anomalies from the mean map value. Top: April. Bottom: July.
Fig. 14 - Differenza tra valori minimi e medi mensili del contenuto d'acqua alla profondità media di 23 cm, anomalie rispetto al valore medio di mappa. Alto: aprile. Basso: luglio.

the 10th percentile (Fig. 15). The July map prompts a geographic pattern which highlights the higher degree of exposure to drought of the central part of Trentino, especially in the comparatively less rainy north.

4. CONCLUSIONS AND DESIRED FUTURE DEVELOPMENTS

The hydrological model GEOtop 2.0 was used to simulate soil moisture in Trentino, a region in the central – eastern Italian Alps, under theoretical conditions of natural water supply (no irrigation). The aim was mainly to perform a modelling of

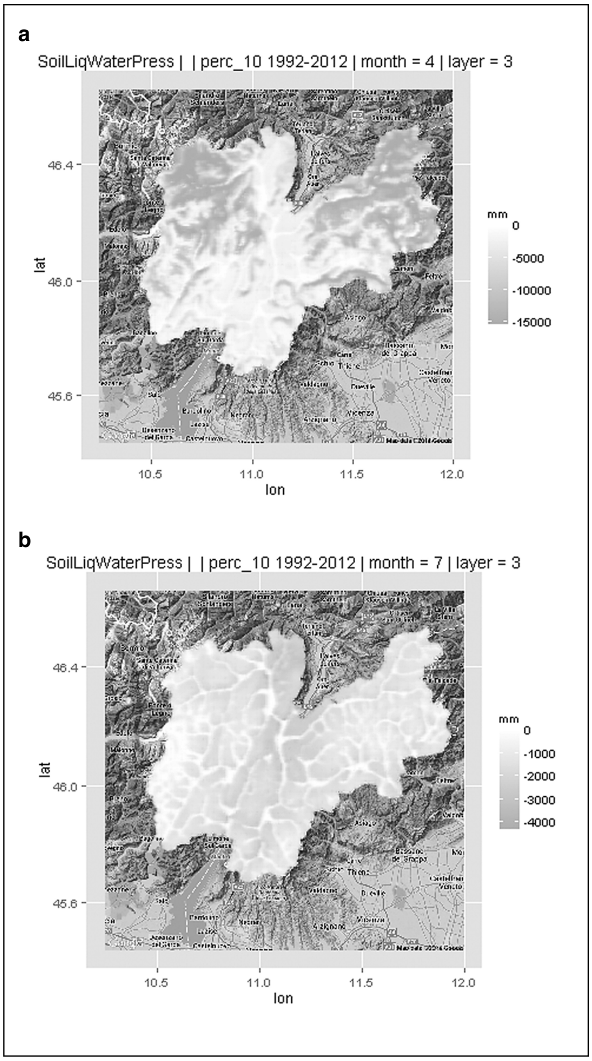

Fig. 15 - Hydraulic pressure load on soil at the mean depth of 23 cm, 10th percentile. Top: April. Bottom: July.
Fig. 15 - Carico di pressione idraulica sul suolo alla profondità media di 23 cm, 10° percentile. Alto: aprile. Basso: luglio.

climatological conditions of soil moisture, also to contribute the wider project of Climate Atlas for Trentino. Simulations were carried out making use of all the meteorological variables available (hourly series). Soil use data were set up according to the information layers given by OpenData Trentino and CORINE Land Use standards.

Results point out that average, natural conditions, typical for each season, are strongly determined by soil features in terms of thickness and retention curves, which, in the implementation described in this work, have been set as uniform all over the domain. This is certainly an important restriction, however, in the current condition of unavailability of detailed and digital pedological information, results point out that, even under the hypothesis of homogeneous soil, some differences can be highlighted in the hydraulic behaviour of soils. This is mainly due to the topographic features, which promote or hampers down valley flow, but also to the different rainfall regimes, and to different evapotranspiration rates (in turn, mainly determined by the thermal gradient, but also by the different vegetation soil cover and by the resulting simulation of meteorological drivers).

A detection of trends, or changes, was sought for the time series of soil water indices. The period when hourly series were available in the area, from early 90s', has limited the time span of the simulation to the 21-year period 1992 – 2012. This did not allow to find important changes in the natural hydraulic regime of soils, given that precipitation have not undergone important changes, particularly in summer (Di Piazza and Eccel, 2012; Eccel *et al.*, 2012), and that the stronger warming period occurred within the late 80s'.

The knowledge of soil moisture conditions can be useful for agrometeorological applications, like control in drought episodes onset (Heim, 2002). But in general, project IdroClima, beyond having assessed a climatological, quantitative overview of water presence in the soils of Trentino, has allowed the creation of the scientific and technical background to apply the model to further simulations, which could encompass:

- other, perhaps wider areas;
- better knowledge of soil properties, which could arise from the creation of a digital pedological map and/or from the creation of a Digital Soil Map (Lagacherie, 2008);
- availability of soil measurements for calibration purposes;
- implementation of climate change scenarios, for comparison with present conditions.

ACKNOWLEDGEMENTS

The authors wish to thank Daniele Andreis (FEM), Giacomo Bertoldi (EURAC), Matteo dell'Amico (Mountain.eering) and Stefano Endrizzi for their support in the use of GEOtop. The IdroClima Project was co-funded by the "Climate Change Fund" – Autonomous Province of Trento, 2012. Thanks to Andrea Cattani (FEM) for his assistance in the computational setup and to Alessandro Biasi (FEM) for the technical support in soil moisture measurement.

REFERENCES

Barontini S., Clerici A., Ranzi R., Bacchi B., 2005. Saturated Hydraulic Conductivity and Water Retention Relationships for Alpine Mountain Soils. In: de Jong, C., Collins, D.N., Ranzi, R. (Eds). Climate and Hydrology in Mountain Areas, ISBN: 978-0-470-85814-1, 101:121.

Bertoldi G., Notarnicola C., Leitinger G., Endrizzi S., Zebisch M., Della Chiesa S., Tappeiner U., 2010. Topographical and ecohydrological controls on land surface temperature in an alpine catchment. Ecohydrology 3:189-204.

Bisaglia M., Cappelletto M., Pasini S., Cimolino A., Baruffi F., Galli A., Marsala V., Scarinci A., Gualdi S., Bucchignani E., Zandonella A., 2011. Implementazione di un modello per la stima del deficit irriguo estivo in alta pianura veneto-friulana e prima applicazione in adattamento ai cambiamenti climatici (Progetto Europeo Life+ Trust). Italian Journal of Agrometeorology, XVI (2):5-14.

Cicogna A., Barbieri S., Michelutti G., Bianco D., 2008. Carte di deficit idrico e giorni di stress idrico in Friuli-Venezia Giulia. 11° Convegno Nazionale di Agrometeorologia, S. Michele all'Adige (TN), 10-12 giugno 2008, Book of Extended Abstracts. Italian Journal of Agrometeorology, 13:106-107.

Cordano E. 2006. Subsurface flow in a catchment: theoretical tools. PhD Thesis. Doctoral School of Fluid Dynamics and Environmental Engineering Processes, Genova.

Damberg L., AghaKouchak A., 2014. Global trends and patterns of drought from space. Theor. Appl. Climatol. 117:441–448. DOI 10.1007/s00704-013-1019-5.

Di Piazza A., Eccel E., 2012. Analisi di serie giornaliere di temperatura e precipitazione in Trentino nel periodo 1958-2010. Provincia Autonoma di Trento e Fondazione E. Mach. 88 pp.

Eccel E., Saibanti S., 2007. Inquadramento climatico dell'Altopiano di Lavarone-Vezzena nel contesto generale trentino. Studi Trentini di Scienze Naturali, Acta Biologica 82:111-121.

Eccel E., Cau P., and Ranzi R., 2012. Data reconstruction and homogenization for reducing uncertainties in high-resolution climate analysis in Alpine regions. Theoretical and Applied Climatology, 110(3):345-358. DOI 10.1007/s00704-012-0624-z

Endrizzi S., Dall'Amico M., Gruber S., Rigon R., 2011. GEOtop Users Manual. Available at www.geotop.org

Endrizzi S., Gruber S., Dall'Amico M., Rigon R., 2014. GEOtop 2.0: simulating the combined energy and water balance at and below the land surface accounting for soil freezing, snow cover and terrain effects. Geoscientific Model Development Discussion, 7:2831-2857.

Endrizzi S., Marsh P., 2010. Observations and modeling of turbulent fluxes during melt at the shrub-tundra transition zone 1: point scale variations, Hydrology Research, 41(6): 471-491.

Ford T.W., Quiring S.M., 2014. Comparison and application of multiple methods for temporal interpolation of daily soil moisture. Int. J. Climatol. 34: 2604-262. DOI: 10.1002/joc.3862

Grossi G., Caronna P., Ranzi R., 2013. Hydrologic vulnerability to climate change of the Mandrone glacier (Adamello-Presanella group, Italian Alps). Advances in Water Resources, 55(190-203).

Heim R.R., 2002. A review of twentieth-century drought indices used in the United States. B. Am. Meteorol. Soc. 83(8):1149-1165.

Jarvis A., Reuter H.I., Nelson A., Guevara E., 2008. Hole-filled seamless SRTM data V4, International Centre for Tropical Agriculture (CIAT), available from http://srtm.csi.cgiar.org.

Lagacherie P., 2008. Digital Soil Mapping: a state of the art. In: Hertemink A.E., McBratney A.B., and Mendoça-Santos M.L. (eds.), Digital Soil Mapping with Limited Data. Springer, Dordrecht.

Liston G., Elder K., 2006. A meteorological distribution system for high-resolution terrestrial modeling (MicroMet), Journal of Hydrometeorology, 7:217-234.

Montagnani L., Maresi G., Dorigatti C., Bertagnolli A., Eccel E., Zorer R., Bertamini M., 2005. Winter depression and spring recovering of photosynthetic function of five coniferous species in the treeline zone of the Southern Alps (Trentino - South Tyrol). Studi Trentini di Scienze Naturali, Acta Biologica, 81:227-244.

Mualem Y., 1976. A new model for predicting the hydraulic conductivity of unsaturated porous media. Water Resour. Res., 12: 513-522.

R Development Core Team, 2008. R: A language and environment for statistical computing. R Foundation for Statistical Computing, Vienna, Austria. ISBN 3-900051-07-0 URL http://www.R-project.org

Reuter H.I, Nelson A., Jarvis A., 2007. An evaluation of void filling interpolation methods for SRTM data, International Journal of Geographic Information Science, 21(9):983-1008.
Rigon R., Bertoldi G., Over T.M., 2006. GEOtop: a distributed hydrological model with coupled water and energy budgets, J. Hydromet., 7:371-388.
Robock, A., *et al.*, 2000. The Global Soil Moisture Data Bank. Bull. Am. Meteor. Soc., 81, 1281-1299.
Seneviratne S.I., Corti T., Davin E.L., Hirschi M., Jaeger E.B., Lehner I., Orlowsky B., Teuling A.J., 2010. Investigating soil moisture–climate interactions in a changing climate: A review. Earth-Science Reviews 99:125-161.
Sheffield J., Wood E.F., 2008a. Projected changes in drought occurrence under future global warming from multi-model, multi-scenario, IPCC AR4 simulations. Climate Dyn., 31:79-105.
Sheffield J., Wood E.F., 2008b. Global Trends and Variability in Soil Moisture and Drought Characteristics, 1950-2000, from Observation-Driven Simulations of the Terrestrial Hydrologic Cycle. Journal of Climate, 21:432:458.
Spinoni J., Naumann G., Carrao H., Barbosa P., Vogt J., 2014. World drought frequency, duration, and severity for 1951–2010. Int. J. Climatol., 34: 2792-2804.
Tabari H., Talaee H., 2014. Sensitivity of evapotranspiration to climatic change in different climates. Global and Planetary Change 115 16-23.
Van Genuchten M.T., 1980. A closed-form equation for predicting the hydraulic conductivity of unsaturated soils. Soil Science Society of America Journal 44(5):892-898.
Vicente-Serrano S.M., Lopez-Moreno J.I., Beguería S., Lorenzo-Lacruz J., Sanchez-Lorenzo A., García-Ruiz J.M., Azorin-Molina C., Morán-Tejeda E., Revuelto J., Trigo R., Coelho F., Espejo F., 2014. Evidence of increasing drought severity caused by temperature rise in southern Europe. Environ. Res. Lett. 9 044001. doi:10.1088/1748-9326/9/4/044001.